

Article citation info:

Dudkiewicz Ł., Hawryluk M., Polak S., Gronostajski Z., Improving process reliability and dimensional accuracy in precision forgings: a comparative study of cold and hot trimming for the automotive industry, *Eksploracja i Niezawodność – Maintenance and Reliability* 2026; 28(2) <http://10.17531/ein/214294>

## **Improving process reliability and dimensional accuracy in precision forgings: a comparative study of cold and hot trimming for the automotive industry**



**Łukasz Dudkiewicz<sup>a,b\*</sup>, Marek Robert Hawryluk<sup>a</sup>, Sławomir Polak<sup>a</sup>, Zbigniew Gronostajski<sup>a</sup>**

<sup>a</sup> Wrocław University of Science and Technology, Department of Metal Forming, Welding and Metrology, Poland

<sup>b</sup> Schraner Polska, Lotnicza 21G, 99-100 Łeczyca, Poland

### **Highlights**

- Comprehensive analysis of the precision cold and hot trimming process.
- Analysis of the impact of the trimming method on overall process reliability.
- Macroanalysis combined with 3D scanning.
- Numerical modeling of the forging and trimming process.
- Operational durability of cold trimming and hot trimming tools.

### **Abstract**

The article presents research on the analysis of the possibility of modifying the hot die forging process by replacing cold trimming with hot trimming. The study examines the effect of this modification on the precision forgings and the improvement of process efficiency and reliability. The research focuses particularly on the impact of the trimming method on overall process reliability, understood as the stability, repeatability, and robustness of the forging operation in industrial conditions. The components are made of austenitic stainless steel and manufactured using a hammer and trimmed using an eccentric press with a pressing force of 105 tons. The research results enabled the selection of the optimal solution for flash trimming—whether cold or hot—taking into account tool durability, the elimination of production bottlenecks and the achievement of high dimensional and shape accuracy of the forgings themselves. The conducted studies confirmed the usefulness and reliability of numerical modelling results for the analysis of one of the forging and trimming.

### **Keywords**

tool durability, process reliability, precision hot forging, tool wear, materials engineering, performance tracking

This is an open access article under the CC BY license (<https://creativecommons.org/licenses/by/4.0/>)

### **1. Introduction**

Precision hot die forging is one of the oldest and most challenging manufacturing processes [1]. It is a widely used manufacturing method due to the high performance of the components produced with it, i.e. forgings. Critical machine and equipment parts are manufactured using this technology [2]. Due to its high functional properties, including mechanical strength, high dimensional and shape accuracy [3], repeatability, favourable fibre orientation, and other advantages, this technology is widely used in the automotive, aerospace and

machinery industries, as well as in the military sector [4,5]. Hot die forging processes at elevated temperatures, which enable the production of components with high operational properties, are typically multi-stage and consist of raw material cutting, hot die forging, cold or hot trimming, heat treatment, shot blasting and straightening of the forgings if required [6]. Developing an optimal technological sequence for manufacturing a given product requires an individual approach—each process must be analyzed separately depending on numerous factors, including

(\*) Corresponding author.  
E-mail addresses:

Ł. Dudkiewicz (ORCID: 0009-0000-0191-7687) [lukasz.dudkiewicz@pwr.edu.pl](mailto:lukasz.dudkiewicz@pwr.edu.pl), M. Hawryluk (ORCID: 0000-0002-9338-4327) [marek.hawryluk@pwr.edu.pl](mailto:marek.hawryluk@pwr.edu.pl), S. Polak (ORCID: 0000-0003-4696-6006) [slawomir.polak@pwr.edu.pl](mailto:slawomir.polak@pwr.edu.pl), Z. Gronostajski (ORCID: 0000-0002-3550-1003) [zbigniew.gronostajski@pwr.edu.pl](mailto:zbigniew.gronostajski@pwr.edu.pl)

the complexity of the forging, the type of input material and the required dimensional and shape accuracy [7,8,9]. Currently, the most popular methods for analyzing, improving and optimizing die forging processes are computer simulations performed through numerical modelling. Numerical modelling software, which consists of computational packages, allows for the simulation of hot forging, cold and hot trimming, billet heating and the cooling of both forgings and billets [10,11]. The most common applications of FEM/FVM-based computational packages include the evaluation of material flow, analysis of contact with the billet by verifying the degree of tool cavity fill, analysis of stress and strain states, as well as the temperature distribution in both the tools and the forgings [12,13]. Hot die forging processes are well known and, due to their complex nature, are the subject of numerous studies [Błąd! Nie można znaleźć źródła odwołania.,15,16]. These processes are carried out using forging units, including hammers and presses. Hydraulic hammers and screw or screw-friction presses are being used increasingly often [17,18]. The process is strongly influenced by several key parameters, such as forging

temperature, tool temperature, type of lubrication, lubricant dosage, lubricant ratio and the method of billet heating. The complexity of the process arises from both the high-temperature conditions and the many interdependent adjustable parameters. In such highly complex and dynamic manufacturing environments, process reliability becomes a decisive factor in ensuring the reproducibility and performance of forgings. Reliability-oriented process design aims to minimize the occurrence of deviations or instabilities resulting from thermal gradients, lubrication variability, or inconsistent billet heating. By integrating predictive analytics and condition monitoring techniques, it becomes possible to proactively mitigate sources of failure and enhance the reliability of both equipment and final products [19,20]. Moreover, despite the ongoing development of technology, including automation and robotics, a large number of forging processes are still carried out manually or semi-automatically [21,22]. Figure 1 shows an example of a process flow diagram for an industrial forging process.

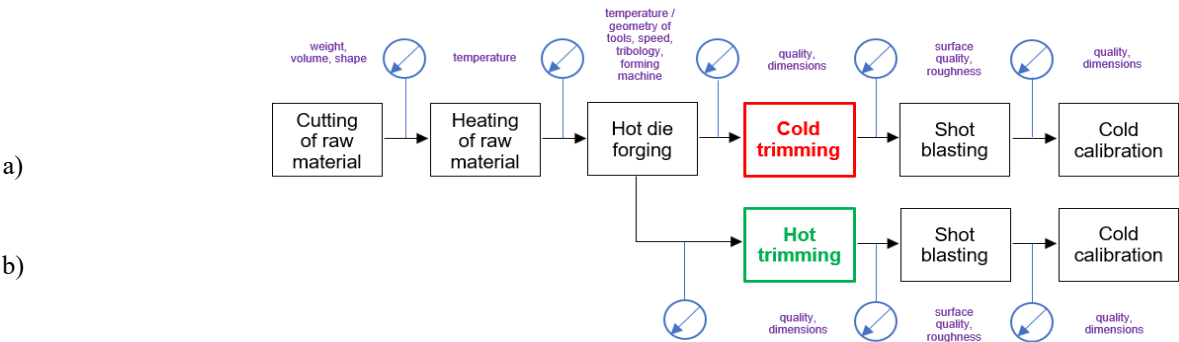


Fig. 1. View of: a) a process flow diagram of an industrial forging process with cold trimming, b) a process flow diagram of an industrial forging process with hot trimming.

Most die forging technologies consist of similar technological process stages, which may differ in sequence, especially after the main forging operation. As can be observed, flash trimming often follows the hot die forging process.

Depending on the technology and the available forging equipment, this operation can be carried out either cold or hot, i.e. directly after forging. The flash trimming process has been shown in Fig. 2.



Fig. 2. View of: a) a diagram of the trimming process, b) the forging with flash before trimming, c) the flash after the trimming process in a single-stage setup.

This process can be carried out through cold or hot/warm trimming. The flash trimming process is also physically and geometrically complex [23]. The purpose of trimming is to even out the edges of the part by removing the excess material left over from the previous operation, i.e. forging. The cut-out (inner) part is the component/forging, while the material outside the cutting line is the flash—scrap material [24]. Trimming involves overcoming the material's cohesion by concentrating stress along the cutting line. The cutting process itself consists of several successive phases as the cutting force increases. In the first phase, mainly elastic deformations and bending of the cut surface occur. When the stresses become high, they cause localized plastic deformation of the material. The second phase involves springback. As the stress continues to increase, the plastic zone penetrates deeper into the material, and the metal flows plastically in the area surrounding the cutting surface. This is the third phase—plastic flow. In the fourth phase, the material loses cohesion and begins to fracture when the stresses reach a critical level [25]. When the optimal clearance between the tools, i.e. the punch and the trimming die, is achieved, fractures from both cutting edges meet, forming a surface contour resembling the letter “S” [26]. To ensure high dimensional and shape accuracy as well as good quality of the cut surface, it is essential to maintain the trimming tools in good condition. The cutting plate must not be dull, and the clearance between the cutting plate and the punch must be optimal. Excessive clearance leads to significant bending of the cut flash edges and results in large burrs on the forging. Too small a clearance can lead to the material jamming between the cutting plate and the punch, which is an undesirable phenomenon [27]. Moreover, in both situations described above, the cutting plate undergoes accelerated wear. For these reasons, the development of a proper trimming tool design, followed by regular and appropriate inspections, is a crucial factor in ensuring the production of high-quality components using these tools [1].

When cold trimming processes are used, forging equipment with significantly higher pressing force is required compared to hot trimming. Nevertheless, cold trimming provides a more precise and repeatable process, which, in turn, allows for the production of forgings with higher dimensional and shape accuracy. The durability of trimming tools used for cold

processes is considerably lower compared to cutting plates used for hot trimming. Tools for hot trimming, made from hot work tool steel, are characterized by much greater operational durability than those used for cold work [28]. However, hot trimming results in lower dimensional and shape accuracy and reduced repeatability of individual products, as the parts cool at different rates after trimming [29,30,31,32].

Access to modern computer tools also enables the implementation of multi-variant numerical simulations of both hot and cold trimming processes. However, numerical simulations of these processes—particularly in the case of geometrically complex products—are time-consuming [33]. Additionally, the use of numerical simulations not only improves process design but also supports reliability engineering by identifying critical failure modes and sensitivity to operational tolerances. In particular, trimming simulations can reveal zones of potential tool overloading or local material failure, enabling more informed decisions regarding tool geometry, material selection and preventive maintenance strategies [34,35].

Conducting a detailed simulation of the trimming operation for a product with a complex shape is challenging due to the complexity of shearing mechanisms or the fracture mechanisms of ductile materials [36]. The available literature includes numerous scientific studies on the trimming process using analytical methods [37], industrial case studies [23], as well as numerical simulations [38]. The wide range of research conducted highlights the complexity of this issue, and the presented scientific publications allow for a more in-depth analysis of the trimming process for various materials and forging geometries [39], confirming that each technological process must be analyzed individually.

The maintenance of tools, including those used in forging and trimming processes, is an inherent element of hot plastic working processes, in which tools are subjected to intensive thermo-mechanical load. In practice, this means the maximum use of dies and cutters in a limited time, leading to their progressive wear - both partial and total. For this reason, issues related to the durability of tools in forging and trimming conditions are widely analyzed in technical literature, and numerous research and development works focus on identifying key factors influencing their durability and on developing

material and technological solutions that allow for extending this durability [40,41].

Ensuring high process reliability is crucial in hot die forging operations. Factors such as tool wear, material inconsistencies, and process parameter variations can significantly impact the consistency and quality of the final products. Implementing robust maintenance strategies and continuous monitoring can mitigate these risks, enhancing the overall reliability of the forging process [42,43]. Moreover, systematic assessment of equipment readiness and component degradation allows for early detection of failure-prone stages, which supports decision-making processes related to tool design, maintenance scheduling, and technology selection [44,45].

**The aim of the conducted research is to analyze the effect of changing the hot die forging technology from a four-stage setup with single-stage cold trimming to a four-stage hot die forging process with single-stage hot trimming on the**

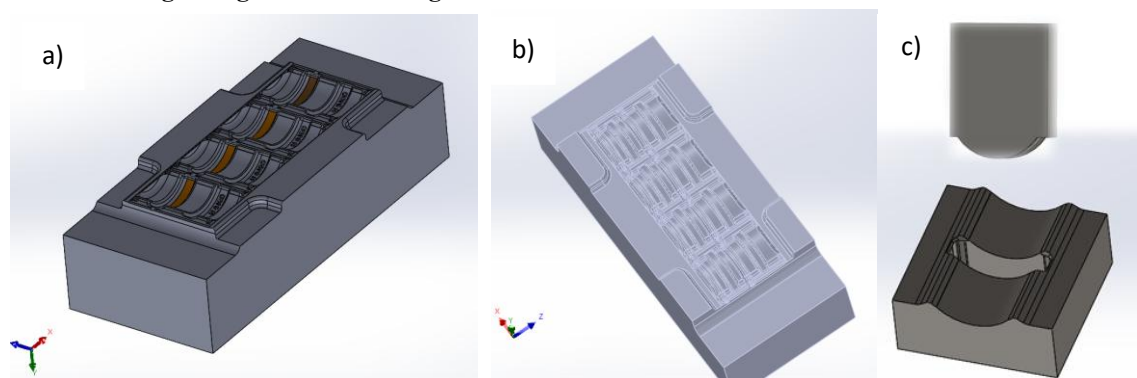


Fig. 3. The view of a 3D model of forging tools: a) lower die, b) upper die, c) deburring tools.

The research was carried out using the following methods and techniques:– analysis of the currently implemented hot forging and cold trimming technology;– numerical modelling of the hot die forging process and both cold and hot trimming using FORGE NxT 3.0 software;– CAD design (SolidWorks 2024);– measurement of tool and forging geometry using a Mitutoyo Strato-Apex 776 coordinate measuring machine, a Mahr XC20 contour measuring device and a TESA height gauge.

## **2.1. Preliminary analysis of the currently implemented four-stage hot forging technology and single-stage cold trimming process**

The technological process is carried out according to a developed and implemented method that enables the production of forgings in a four-stage setup during hot forging and single-stage cold trimming. Both the forging and trimming

**process efficiency and the dimensional and shape accuracy of forgings made of stainless steel.**

## **2. Research subject and methodology**

The subject of the research is the hot die forging and cold trimming process used to produce ring segment-shaped forgings. The forgings are made of AISI 304 austenitic stainless steel. The ring segment forging process is carried out using a LASCO hammer with an impact energy of 16 kJ. The forging dies are made from material 1.2344. The tools are preheated to a temperature of 200°C. Cold flash trimming is performed on a MIOS press with a pressing force of 105 t. The flash trimming tools are made of K110 cold work tool steel.

Fig. 3a,b shows the view of the tools used for the four-stage forging process in the current technology, while Fig. 1c illustrates the flash trimming tool used in the single-stage setup.

processes are conducted manually. Forging is performed on a hydraulic hammer, while trimming is carried out on an eccentric press. The produced forgings are intended for critical machine parts in the automotive industry and therefore require a carefully planned control strategy and strict in-process inspections to ensure repeatability and stability of the manufacturing processes. The forgings in question are made from AISI 304, an austenitic stainless steel. The mass of a single forging after the trimming process is 37 g. The input material for the forging process consists of round bars cut to the appropriate length. In this form, the material is transferred to the next technological operation, i.e. hot die forging.

The hot die forging process is carried out in two seats: the roughing pass and the finishing impression. The technology involves one blow in the roughing pass (1X) and one blow in the finishing impression (2X). Manual lubrication of the forging



tools is applied during both stages—roughing pass (1X) and finishing impression (2X). The used lubricant is Graphitex 289 in a 1:10 ratio. The forging temperature is 1165°C and the cycle time is 12 seconds. A detailed analysis of the forging tools and additional information about the forging process can be found

in [41]. The technology for manufacturing forgings intended for window fitting components (Fig. 2) is carried out on a hydraulic hammer (Fig. 4) through the process of hot forging in an open die, across two stages: roughing and finishing dies, and the forgings are produced in multiple systems.

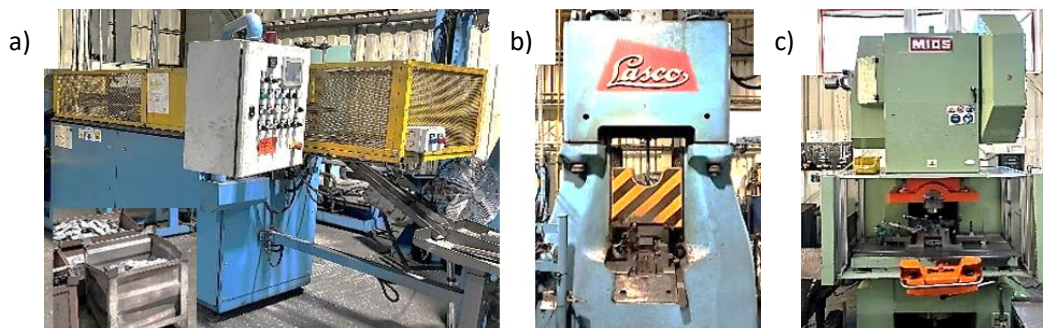


Fig. 4. The photos of a semi-automated production line, consisting of: a) a 125 kW induction heater, b) a double-acting hydraulic forging hammer with an energy output of 16 kJ, and c) an eccentric press for trimming flash with a force of 1 MN.

This process yields a larger component known as a 'leaf,' from which six individual forgings with pin-like protrusions, perpendicular to the main axis, are simultaneously produced. These forgings are challenging to manufacture due to their complex shape and the precise dimensional and form tolerances required (low tolerances of 0.15 mm, radii of 0.5 - 1 mm). The

forged 'leaf' with its individual forgings forms a slender, long, and thin element. The forging tools are made from steel 1.2344, with a hardness of approximately 52 HRC, and are heated to an operating temperature of around 140-180°C. To analyse and verify the implemented technology, a temperature distribution analysis of the forging tools was conducted (Fig.5).

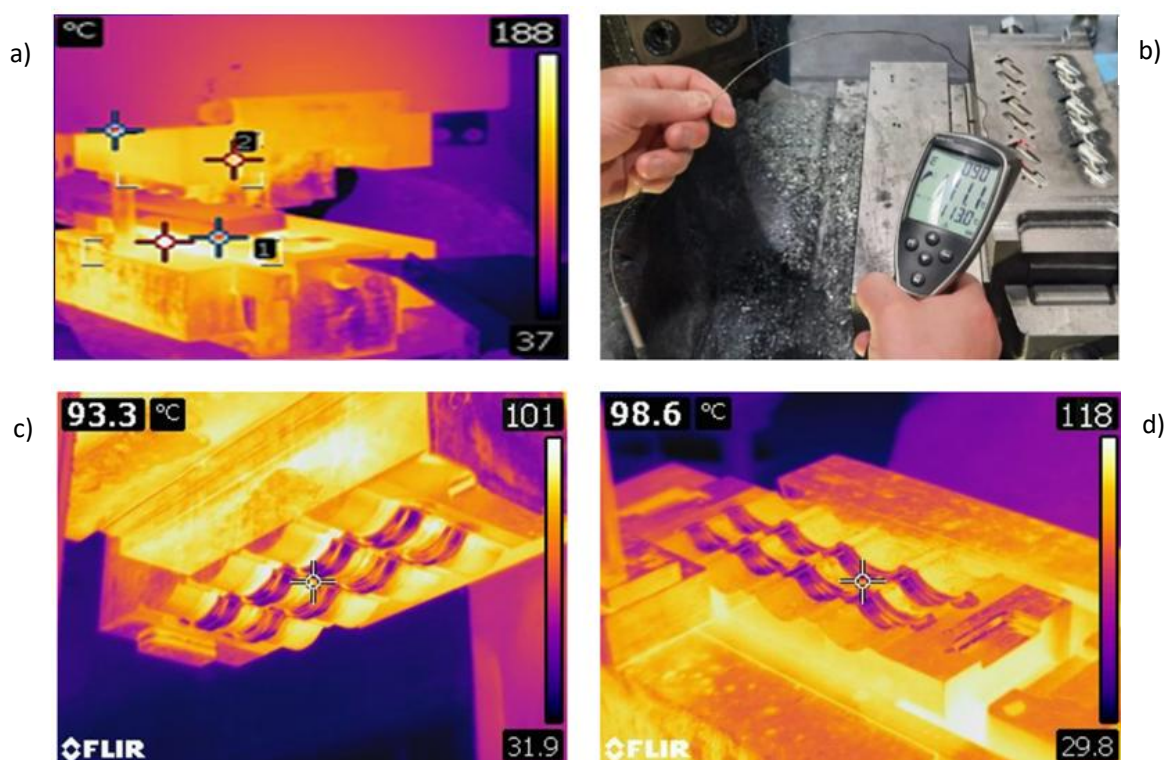


Fig. 5. Temperature measurement results for the tools include: a) a thermographic image showing the temperature distribution on the dies immediately after heating for the forging process, b) temperature measurements on the lower die using a pyrometer and thermocouple to verify the readings obtained from the thermal imaging camera, and a detailed analysis of the temperature field for both dies c) upper die, d) lower die.

To verify the temperature measurements obtained using a thermal imaging camera, a pyrometer and thermocouple were employed (see Fig. 3a,b,c). These methods showed good agreement, thereby validating the use of thermal imaging for temperature assessment. The analysis of the results indicates that the average temperature of the upper die is approximately 170°C, while the lower tool maintains a temperature of around 140°C. According to the technological assumptions, such temperature distributions are correct, as there is a tendency over time for the upper tool to cool and the lower tool to heat up. This is due to the varying contact durations with the hot workpiece and forging. The technology stipulates that if the temperature of the upper die drops to approximately 100°C, the process must be halted to reheat both tools. Only continuous control of key parameters of the technological process can ensure stable and repeatable conditions, which will translate into correct forgings, which after forging are cooled in air and passed on to further machining processes, including cold trimming.

The cold flash trimming process is carried out after the forgings produced during hot die forging have been cooled. The main purpose of this operation is to separate the flash, which constitutes scrap, from the final forging. This operation is performed in a single-stage setup, meaning the operator trims a leaf (consisting of four individual forgings) by separating the final products from the flash surrounding the four pieces in a single step. Since the process is performed cold, it is characterized by very high repeatability and excellent surface quality after trimming. The average tool life for the forging process tooling is approximately 3294 forgings, as shown in Table 1. Detailed information on the durability of the forging tools can be found in [41].

Table 1. Durability of forging tools according to the standard technology [41]

No. of forging tool set	Tool durability (pcs)
	Standard production process
1 <sup>st</sup> set	3 380
2 <sup>nd</sup> set	3 200
3 <sup>rd</sup> set	3 150
4 <sup>th</sup> set	3 400
5 <sup>th</sup> set	3 340
Average	3 294

In the case of cold flash trimming tools, the average tool life was determined based on five sets of cold trimming tools and

has been presented in Table 2.

Table 2. Durability of cold flash trimming tools

No. of forging tool set	Operational durability (pcs)
1 <sup>st</sup> set	15 430
2 <sup>nd</sup> set	16 200
3 <sup>rd</sup> set	15 200
4 <sup>th</sup> set	15 743
5 <sup>th</sup> set	15 362
Average	15 587

As the forging tools wear, the geometry of their working impressions changes, as shown in [23], due to destructive mechanisms. The most intensive wear that affects the subsequent technological process occurs in the material transition zone to the flash, specifically in the bridge area. Moreover, with ongoing tool use, the flash thickness also increases. This, in turn, has a significant effect on the operational durability of the flash trimming tools by enlarging the trimming contour and dulling the cutting edge. As a result, dimensional changes in the forging's outer profile occur, and in extreme cases, forgings may be produced outside the technical specification. The first key issue is the increased flash thickness resulting from wear in the bridge area of the forging tools, where intensive material flow takes place from the working impression into the flash cavity. The growing flash thickness leads to significantly higher forces during trimming, which consequently accelerates the wear of the trimming die and, in extreme cases, causes chipping that renders the tool unusable for further production. Figure 6a shows the forged complete element after the four-stage forging process, and Figure 4b presents the forgings after the trimming process. In the current industrial process, cold trimming is carried out one forging at a time by repositioning the forged element and trimming each piece individually. This approach is dictated by the high cutting forces involved, which make it impossible to perform cold trimming on four forgings simultaneously. The flash after the trimming operation has been shown in Figure 6c.



Fig. 6. View of the forging: a) after the four-stage forging process (forgings with flash), b) after flash trimming, c) view of the flash after the trimming process of the four-stage forgings.

The analyzed forging process for the automotive industry, involving the production of ring segment-shaped forgings, allows for an average operational tool life of approximately 3 250 forgings in the four-impression setup, which corresponds to about 13 000 individual forgings. The average tool life for

single-stage cold flash trimming tools is around 15 000 forgings. When initiating the production process with new tools for forging and cold trimming, the process follows the sequence shown in Fig. 7.

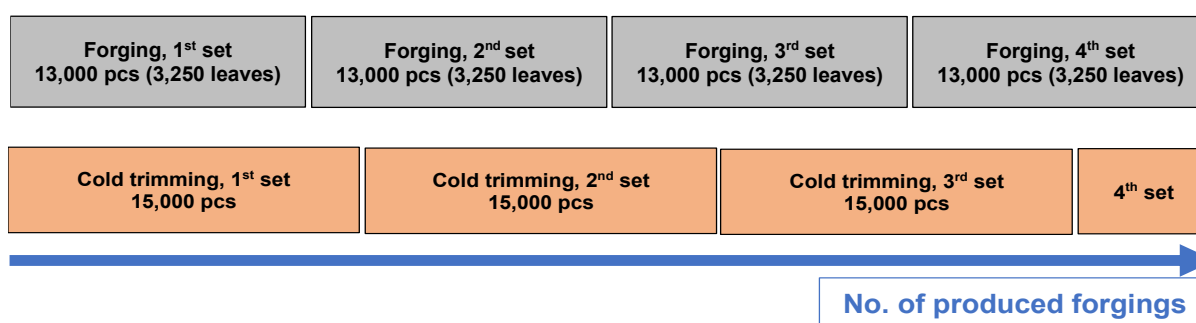


Fig. 7. Manufacturing process using new tools for forging and cold trimming.

As seen in Fig. 7 above, the operational durability of cold trimming tools is significantly higher than that of hot forging tools—by more than 15%. As a result, the process must be halted to replace the tools with new ones—both forging and cold trimming tools—at different time intervals. This leads to interruptions during the production process, which reduces its efficiency and affects the stability and repeatability of the manufacturing process.

## 2.2. Numerical analysis of the currently implemented four-stage forging technology and single-stage trimming process

At this stage of the study, a numerical analysis of the hot die forging process and cold flash trimming was conducted. The numerical simulations were performed using FORGE NxT 3.0 software and the assumed initial and boundary conditions. The

forging tools used in the forging process were subjected to numerical modelling. The forming conditions are consistent with the parameters of the LASCO HO-U 160 hammer and the process specifications outlined in the technological sheets. Detailed parameters in this regard can be found in [41]. The tribological conditions were set according to the Tresca friction model with a factor of 0.35 for all working surfaces of the tools. The Forge program utilizes the following equation for the advanced Tresca friction model:

$$\vec{\tau} = \bar{m} \frac{\sigma_0}{\sqrt{3}} \frac{\Delta \vec{v}}{||\Delta \vec{v}||} \quad (2.1)$$

where:

$\vec{\tau}$  - shear traction vector (also referred to as the frictional shear stress vector)

$\bar{m}$  – is the friction factor ranging from 0 to 1;

$\sigma_0$  – von Mises stresses;

$\|\Delta \vec{v}\|$  – relative sliding velocity.

The heat transfer coefficients between the charge material and the tool, as well as with the environment, were set at 25 and 0.35 kW/m<sup>2</sup>K, respectively. The Forge software employs the Norton-Hoff viscoplastic flow law as its constitutive equation<sup>36</sup>. The general form of this law is as follows.

$$\sigma = 2K \left( \sqrt{3} \frac{\dot{\epsilon}}{\epsilon_i} \right)^{m-1} \epsilon \quad (2.2)$$

The coefficient **m** can take the following values: -  $m = 1$  corresponds to a Newtonian fluid with viscosity  $\eta = K$ , -  $m = 0$  gives the law of plastic flow for a material that meets the Huber-Mises-Hencky plasticity criterion

$0 < m < 1$  for steel deformable on hot.

Where:

$\sigma$  – true (or effective) stress, [MPa]

$K$  - material strength coefficient (a temperature-dependent material constant), [MPa]

$\epsilon_i$  - equivalent plastic strain rate (also called the effective strain rate), [1/s]

$\dot{\epsilon}$  - strain rate, [1/s]

$m$  - strain rate sensitivity exponent (describes how stress changes with strain rate), dimensionless

$\sqrt{3}$  - coefficient resulting from the von Mises yield criterion in plasticity theory

For most metals, the parameter **m** falls within the range of 0.1 to 0.2.

The material model for forging (AISI 304 steel) was sourced from the Forge software database "FPD Base 1.3" and is represented using the Spittel equation in the form (2.3):

$$\sigma_f = A e^{m_1 T} T^{m_9} \epsilon^{m_2} e^{\frac{m_4}{\epsilon}} (1 + \epsilon)^{m_5 T} e^{m_7 \epsilon} \epsilon^{m_3} \epsilon^{m_8 T} \quad (2.3)$$

The specific coefficients in the equation for the cold and hot process are calculated and selected automatically in the program.

### 2.2.1. Initial and boundary conditions adopted for the numerical calculations of the forging process:

- Charge material diameter:  $\varnothing 12$  mm, charge material length: 276 mm;
- Number of blows: 2, blow parameters: 1X (roughing pass): 12.5 kJ – 1 blow, 2X (finishing impression): 5.5 kJ – 1 blow;

- Forging temperature and cycle time: 1165°C; 12 s, operations during the cycle: cooling – 6 s, forging in the roughing pass – 3 s, forging in the finishing impression – 3 s, tool temperature: 200°C; lubrication: water-based graphite solution;
- Heat transfer: average 10 kW/(m<sup>2</sup>·K);
- Forging temperature and cycle time: 1165°C; 12 s, operations during the cycle: cooling – 6 s, forging in the roughing pass – 3 s, forging in the finishing impression – 3 s, tool temperature: 200°C; lubrication: water-based graphite solution;
- Heat transfer: average 10 kW/(m<sup>2</sup>·K).

### 2.2.2. Numerical analysis of the single-stage cold trimming process

The flash trimming tools used in the single-stage cold trimming process were subjected to numerical modelling. The forming conditions are consistent with the parameters of the MIOS T105TR press with a pressing force of 105 tons and the process specifications outlined in the technological sheets.

Initial and boundary conditions adopted for the numerical calculations of the forging process:

- forging temperature: ambient temperature, 20°C;
- tool temperature: ambient temperature, 20°C;
- friction coefficient for hot forging:  $\mu=0.25$ ;  $m=0.45$ , and for cold trimming:  $\mu=0.15$ ;  $m=0.3$ ;
- heat exchange: average of 10 kW/(m<sup>2</sup>·K);
- clearance during trimming: nominal.

In the case of cold trimming, the Coulomb friction model with a coefficient of 0.4 was adopted, as recommended by the software. The Forge NxT program allows for simulating the material separation process according to two fracture criteria: Oyane and Cockcroft-Latham. In the simulations of the flash trimming process, the normalized Cockcroft-Latham criterion was used, which is expressed by the formula:

$$C = C_0 + \int_0^{\bar{\epsilon}} \Sigma d\bar{\epsilon} \quad (2.4)$$

$$\Sigma = \frac{\sup(\sigma_1, \sigma_2, \sigma_3)}{\sigma_i} \quad (2.5)$$

Where:

**C** – cumulative damage or tool wear indicator (e.g., accumulated fatigue, volumetric wear).

**C<sub>0</sub>** – initial damage/wear value (often assumed to be zero at



the beginning of the process).

$\bar{\epsilon}$  – effective strain (sometimes referred to as equivalent plastic strain).

$\Sigma$  – a degradation function or parameter reflecting local process conditions; it may depend on temperature, stress, strain rate, or microstructural state.

$\int_0^{\bar{\epsilon}} \Sigma d\bar{\epsilon}$  – the cumulative damage or wear resulting from plastic deformation, integrated over the effective strain.

The Cockcroft–Latham criterion is a widely used model for assessing the risk of fracture during plastic deformation of a material, based on the analysis of tensile stresses and total strain. The normalized value of the Cockcroft–Latham criterion, which influences the shape and profile of fractures, the maximum force, and local deformation, can be set between 0 and 1. For cold cutting processes, the Forge program recommends a value between 0.2 and 0.4. Based on numerous simulations corroborated by industrial observations, it was determined that the best results for the trimming process were achieved with a Cockcroft–Latham criterion value of 0.7 (hot) and 0.3 (cold). This was accompanied by adjusting node positions near the cutting line and mapping state variables from the original mesh to a new mesh<sup>3</sup>. For accuracy in material separation simulations, it is crucial that elements along the cutting line are minimized. Tetra elements were used in modeling, with an average count of approximately 438 000 elements for each modeled variant, considering increased local density. The average computation time on an 8-processor license on a standard PC workstation was about 105 hours. The trimming simulation was carried out for the current technology, where this process is performed cold. Therefore, the geometry of the forging after the shaping process was transferred to the

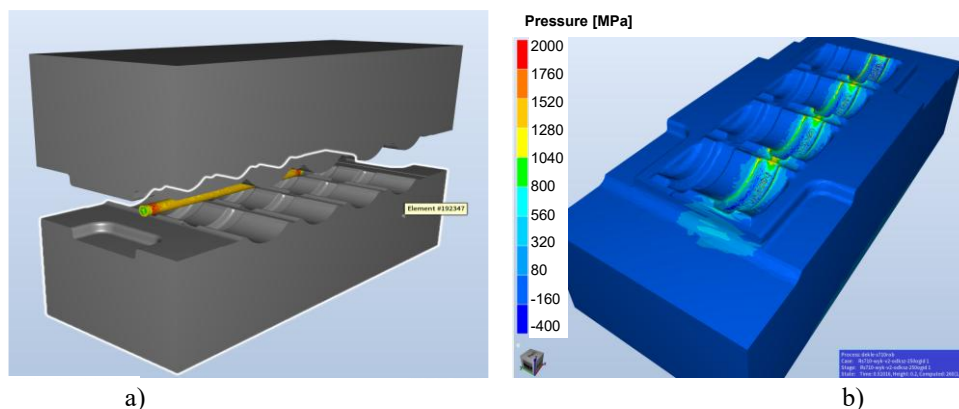
cold trimming simulation. The temperature in the simulation was 20°C. All external loads, as well as the stress and strain fields, were reset. The tools for hot flash trimming used in the single-stage trimming process were designed and subsequently subjected to numerical modelling. The forming conditions are consistent with the parameters of the MIOS T105TR press. The initial and boundary conditions adopted for the numerical calculations of the trimming process are as follows:

- forging temperature: the temperature after the finishing forging operation was assumed, without any inter-operational cooling;
- tool temperature: 250°C;
- friction coefficient for hot forging and hot trimming:  $\mu=0.25$ ;  $m=0.45$ ;
- heat exchange: average of 10 kW/(m<sup>2</sup>·K);
- clearance during trimming: nominal.

In the hot trimming model, the geometric results after forging were transferred along with the temperature field distribution—assuming that the trimming process would be carried out immediately after forging without inter-operational cooling. Since the material is more ductile at higher temperatures, a fracture criterion of 0.7 was applied for the hot trimming process, whereas for the cold trimming operation, it was 0.3. These assumptions were derived from literature regarding simulations of material cutting processes at different temperatures using the Cockcroft–Latham criterion.

### 3. Results and discussion

Figure 8 shows the upper and lower forging tools used in the four-stage forging process, along with the sample results for pressure distribution during forging (Fig. 8a and 8d) and temperature distribution (Fig. 8c).



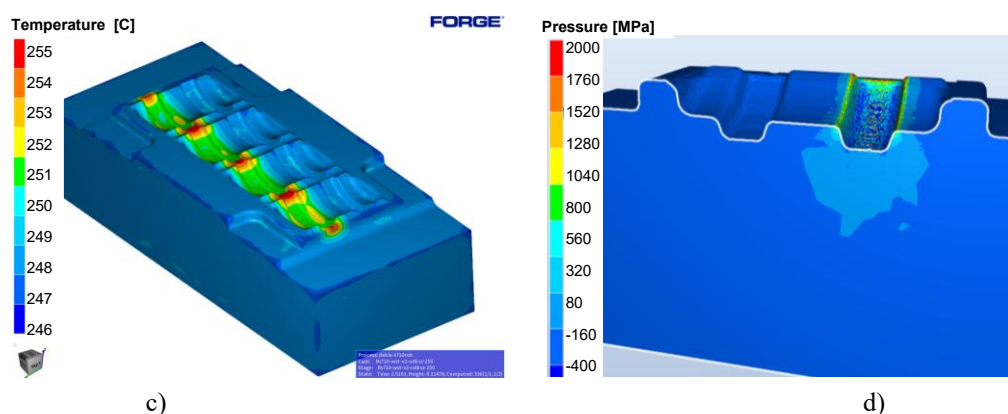


Fig. 8. Numerical modelling results: a) view of the four-stage forging process setup; b) pressure distribution over the entire lower die; c) temperature field variation 2 seconds after the end of forging for 1X; d) pressure distribution on the lower die in cross-section.

To fully analyze the stress distribution in the dies, finite elements were applied to the tools to better reflect the internal pressure distribution acting on the forging dies as well as on individual impressions (Fig. 8b,d). In the working impressions, the highest temperatures occur at the bridges (310°C), while within the impressions themselves, the temperature reaches approximately 240°C. It is important to note that just 2 seconds

after forging (Fig. 8c), the temperature in the entire tool drops by about 50–60°C, which, in an industrial process, can significantly affect the surface layer of the tool. Figure 7 shows the successive steps of the forging process during the roughing pass operation: Fig. 9a – 10 mm before die closure, Fig. 9b – 1 mm before die closure, Fig. 9c – die closure.

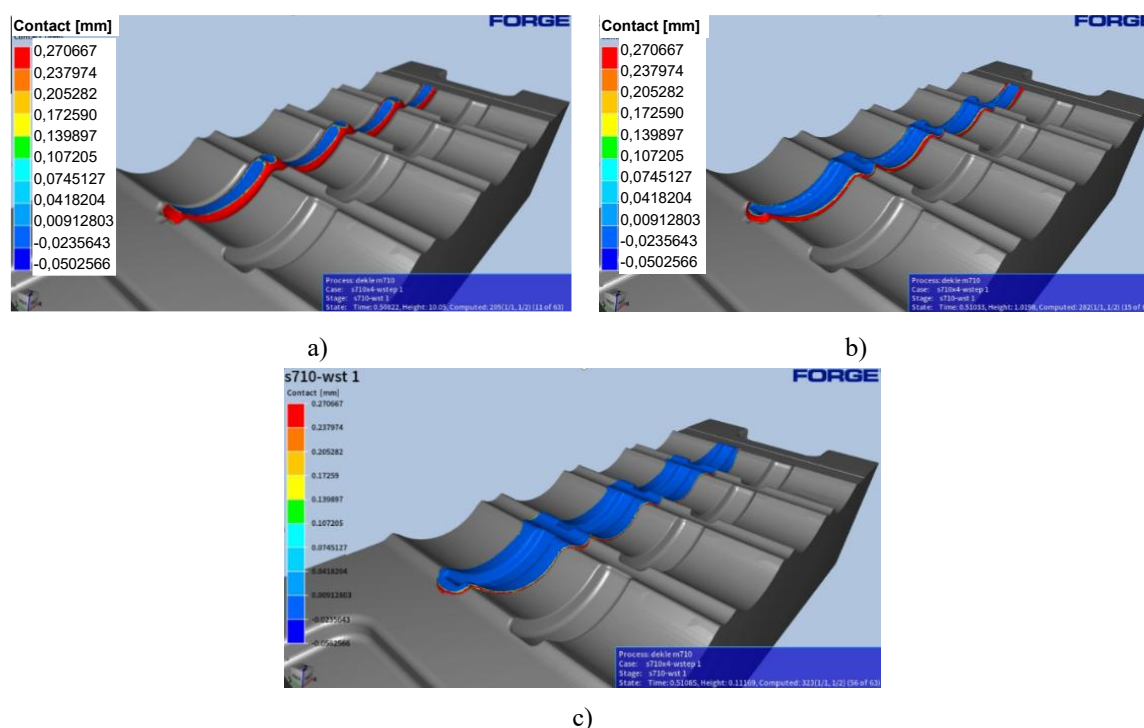


Fig. 9. Successive steps of the S710 forging process simulation – roughing pass operation (blue color indicates contact with the tool), height to contact upper with lower die a) 10 mm, b) 1mm, c) 0.1 mm.

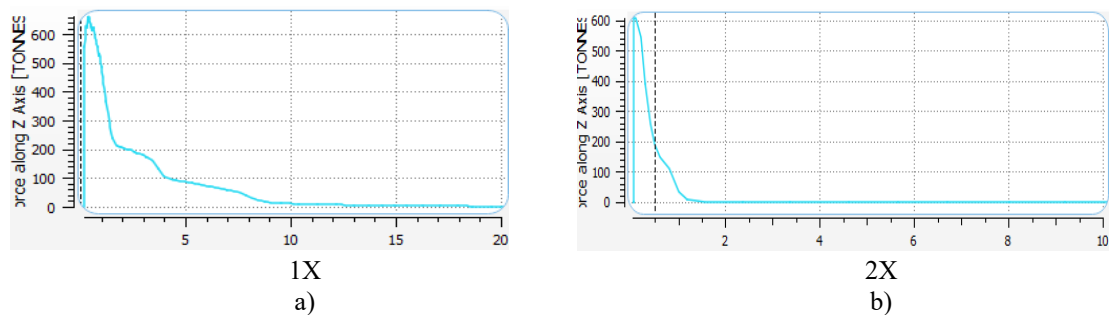


Fig. 10. Forging force in the process: a) roughing pass operation 1X, b) finishing impression operation 2X.

Figure 10. shows the forging force courses in the process for both impressions: Fig. 10a for the roughing pass (1X) and Fig. 8b for the finishing impression (2X).

The maximum load in the roughing pass operation (1X) and the finishing impression operation (2X) is similar and amounts to approximately 600 tons, which should not pose a problem for the overall stress resistance of the tools. The results obtained

from the numerical simulations—regarding die cavity fill, temperature distribution, and force curves for the actual forging process—were confirmed under industrial conditions. Fig. 11a shows the geometry setup in the trimming process, i.e., the knife, cutting plate and forging, while Fig. 11b presents a sample distribution of plastic deformation just before the material separation.

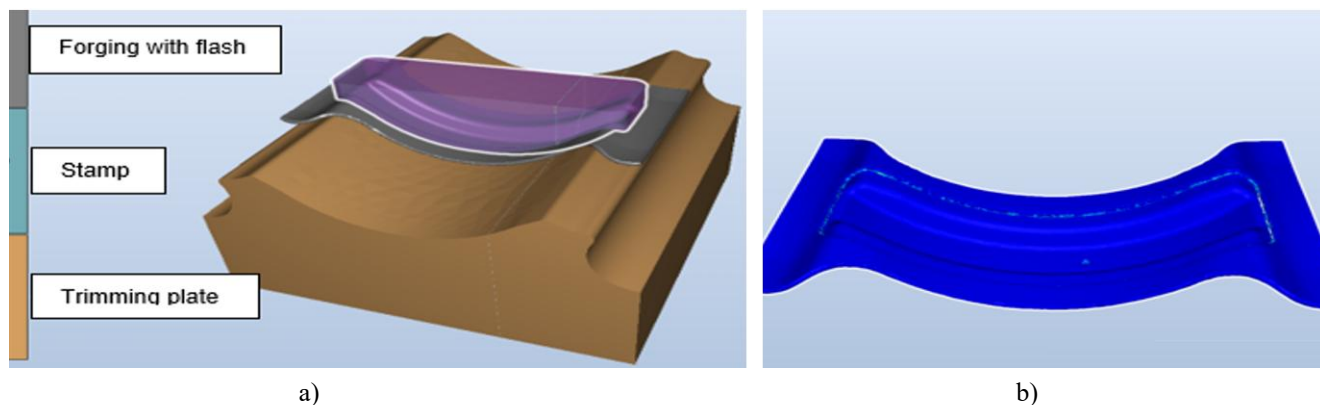


Fig. 11. FE numerical results: a) tool setup for cutting the part, b) forged part.

Due to the long computation time during the cold trimming simulation, a symmetrical setup was adopted by dividing the forging along the symmetry plane along the longer, curved axis of the forging, thus creating  $\frac{1}{2}$  of the forging in a longitudinal

cross-section.

Fig. 12 shows the results of the cold trimming simulation for half of the model, including the temperature field distribution before the process (Fig. 12a) and after cold trimming (Fig. 12b).

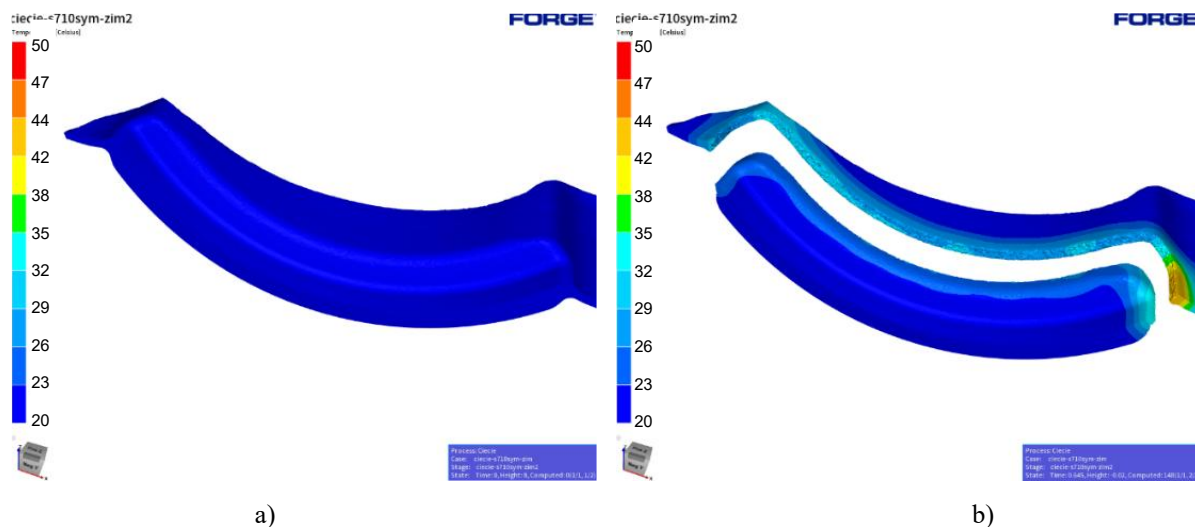


Fig. 12. Numerical simulation results with temperature field distributions: a) before trimming, b) after flash trimming.

As can be observed in the results of the trimming process, both friction and plastic deformation occur, causing a slight increase in temperature (about 20°C), particularly along the cutting line at the ends of the forging. Fig. 12a presents the simulation results for the distribution of equivalent stresses (von Mises) at the final stage of cutting—just before material

separation, while Fig. 12b shows the results related to the applied fracture criterion, illustrating the geometric changes and the moment of material separation. These assumptions were derived from literature concerning simulations of material trimming processes at different temperatures, using the Cockcroft-Latham criterion.

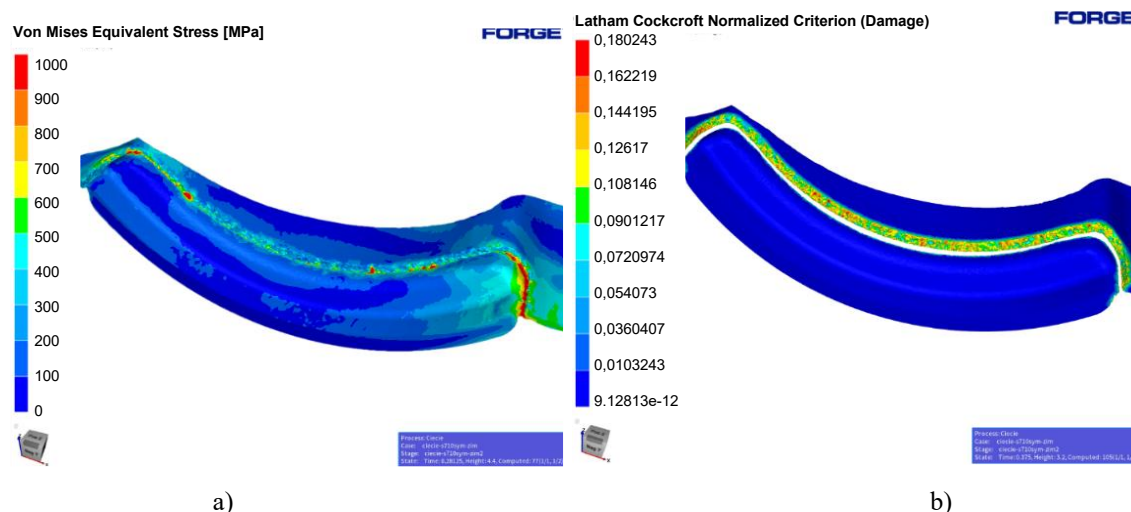


Fig. 12. Numerical simulation results with distributions: a) equivalent stresses at the final stage of cutting, b) temperature field: a) before cutting, b) after flash trimming.

The analysis of the obtained results showed that the highest values of equivalent stresses during the cold trimming process are located along the cutting line, especially at the ends of the forging, where they exceed 1000 MPa. Similarly, the distribution of the CL coefficient shows that the highest values

are also located along the cutting line. The cutting force, as shown in Fig. 13, in the cold simulation is 13 tons for a single forging. This result should be treated as an indicative qualitative measure rather than a quantitative one.

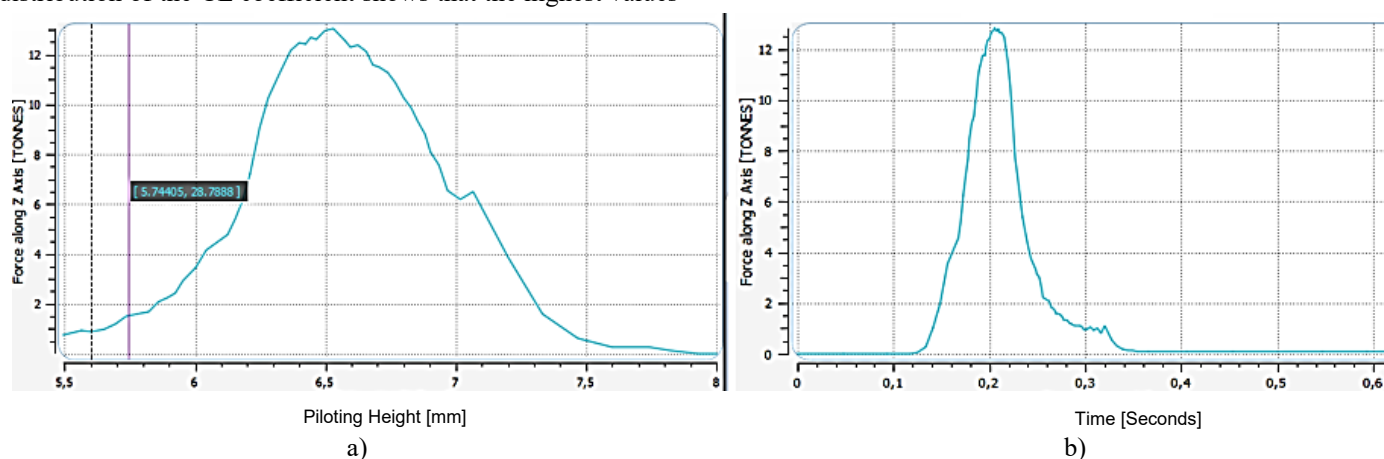


Fig. 13. Cold cutting force course for the part, a) piloting height, b) time.

The peak value rises and falls around 6.5 mm, which corresponds to the time of maximum force for 0.2s in the numerical simulation. A hydraulic press was assumed for the trimming process. High force values during cold trimming can lead to premature wear of the trimming tools.

### 3.1. Verification of numerical simulations under industrial conditions – technological trials

In order to confirm and verify the obtained results, a hot forging and cold trimming process was conducted under industrial conditions. The forging process was carried out on a hammer with an impact energy of 16 kJ, and the flash trimming

was performed on an eccentric press with a pressing force of 105 tons. From the produced trial series, 5 pieces of forgings in the form of leaves were collected after the forging process, selected every 20 pieces, and then measured after flash trimming (a total of 20 final forgings).

### 3.1.1. Qualitative measurements of forgings after the hot forging process

In order to create a representative image of the deformation of the analyzed group of forgings, a measurement process was

carried out for the test batch of forged leaves and individual forgings after the trimming process.

As a result of 3D scanning of the leaves, measurement data was obtained and analyzed using GOM software. To show the deformation, the measurement data alignment process was performed, and the data was aligned on the second seat of the leaf. Fig. 14 shows three sample results of 3D scanning of a representative forging leaf in the form of a color deviation map describing the geometry deformation.

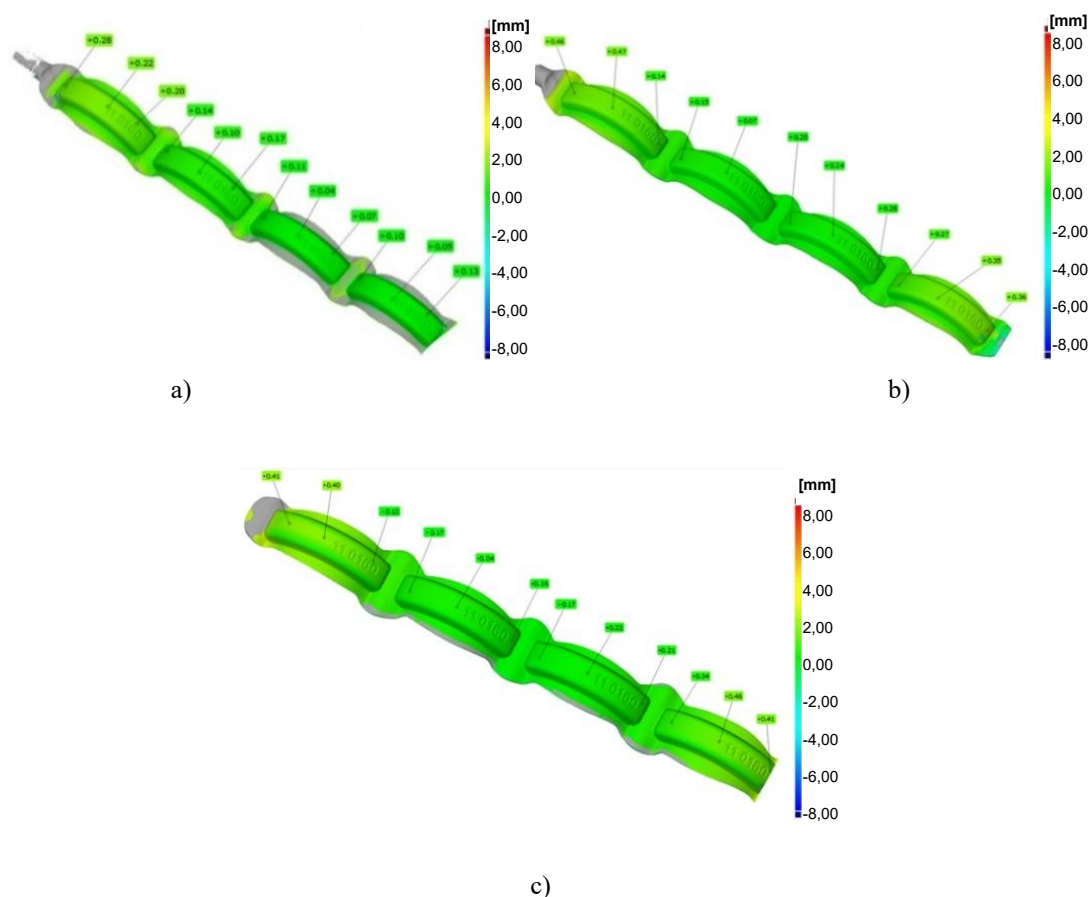


Fig. 14. 3D scanning result of the forging before trimming - top view (a,b,c).

The results shown in Fig. 14 demonstrate the shape repeatability of the forgings. Analyzing the 3D scanning results of the forging for the selected seat measured on the leaf, it can be observed that there are very small surface deformations on each of these forgings compared to the nominal target value. A closer examination reveals a deviation ranging from 0.05 mm to a maximum of 0.46 mm (which results from the leaf warping during cooling after forging). It is important to emphasize that the observed deformations are minimal and remain within acceptable standards. Therefore, it is recommended to conduct additional measurements for selected geometric features to

better understand the effect of this deformation on the functionality and usability of the forgings under specific operating conditions.

### 3.1.2. Qualitative measurements of forgings after the cold trimming process

The forgings taken from the same process were subjected to the cold trimming process Fig. 15a, and next 3D scanning measurements were performed, and example results for the first three forgings are shown in Figs. 15b–15d.



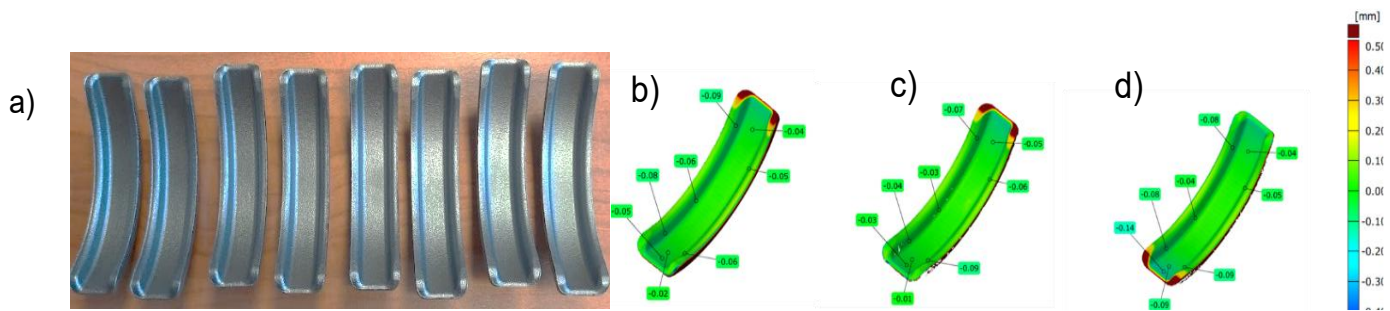


Fig. 15. The view of: a) forging after cold trimming, b) selected 3D scanning results of forgings after cold trimming compared to the nominal model: b) forging no. 1, c) forging no. 2, d) forging no. 3.

The results presented in Fig. 15 for the 3D scanning of forgings from the selected seat after trimming show that each of these forgings exhibits minimal surface deformations compared to the nominal target value. An interesting aspect is the positive effect of the trimming process on the obtained results. A more detailed analysis reveals a deviation ranging from -0.14 mm to a maximum of 0 mm. It should be emphasized that the observed deformations remain within acceptable standards. Additional microstructural tests performed for comparison purposes

revealed a fine-grained austenitic structure (Fig. 16). The structural inhomogeneity is minimal. Various types of secondary particles were present, which were analyzed and identified as particles rich in Cr, Ti, and Mo, with an average size of up to 5  $\mu\text{m}$ . The structure also contains relatively large particles rich in Ti, identified as titanium carbonitrides (TiCN), with an average size of 10-15  $\mu\text{m}$ . No additional layer was observed on the surface of the forgings, indicating a properly conducted hot forging process followed by cold trimming.

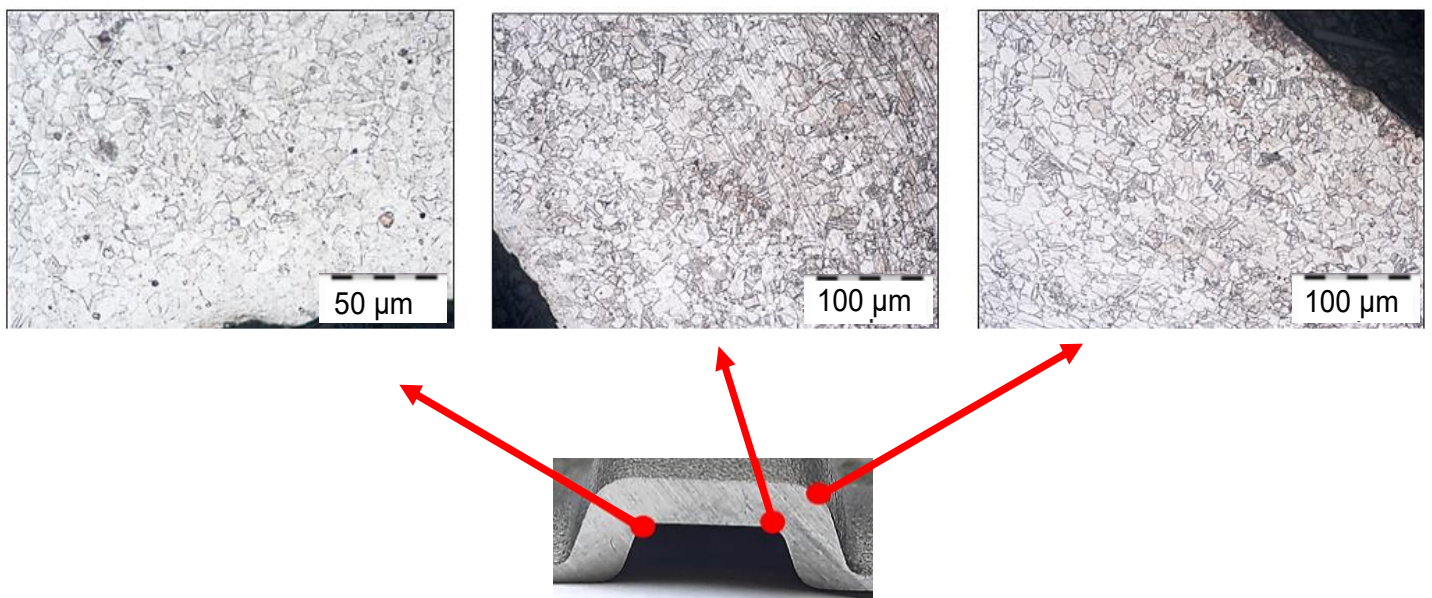


Fig. 16. Microstructure of a stainless steel forging.

Comprehensive tests of cold-trimmed forgings have shown that they are within the specified dimensional tolerances and have the required parameters related to the microstructure. Based on the positive results obtained, it was decided to proceed with numerical simulations for the hot trimming process.

### 3.2. Numerical simulations of hot flash trimming in a single-stage setup

Fig. 17 shows the results of the cold trimming simulation for

half of the model, including the temperature field distribution before the process (Fig. 17a) and after cold trimming (Fig. 17b).

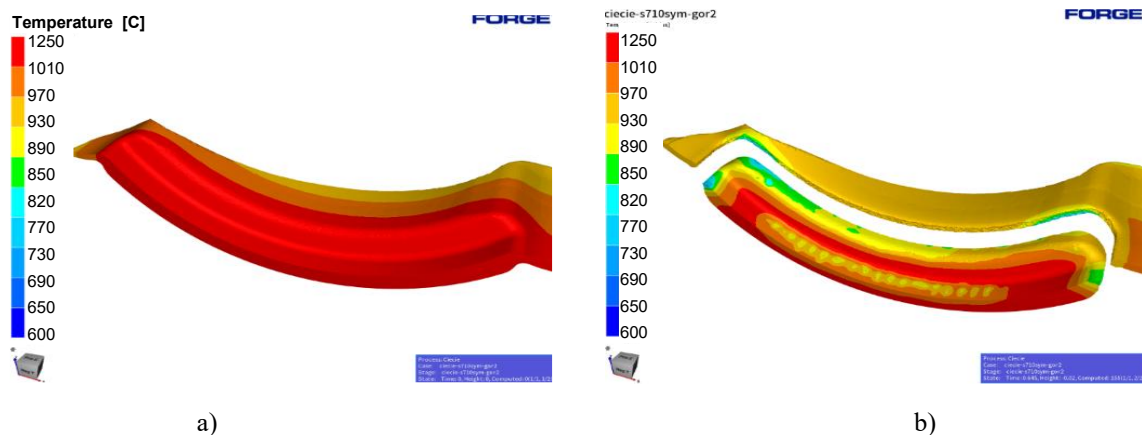


Fig. 17. FEM results with temperature field distributions: a) before trimming, b) after flash trimming.

In the case of hot trimming, similar to cold trimming, both friction and plastic deformation are observed, which should promote an increase in temperature. However, the amount of energy supplied in this way is too small, and in the hot trimming process, the temperature decrease and heat dissipation dominate, especially in the thin flash, where the temperature drops from

1050°C at the beginning to around 800-850°C along the cutting line. Fig. 18a presents the simulation results for the distribution of equivalent stresses (von Mises) at the final stage of cutting—just before material separation, while Fig. 18b shows the results related to the applied fracture criterion, illustrating the geometric changes and the moment of material separation.

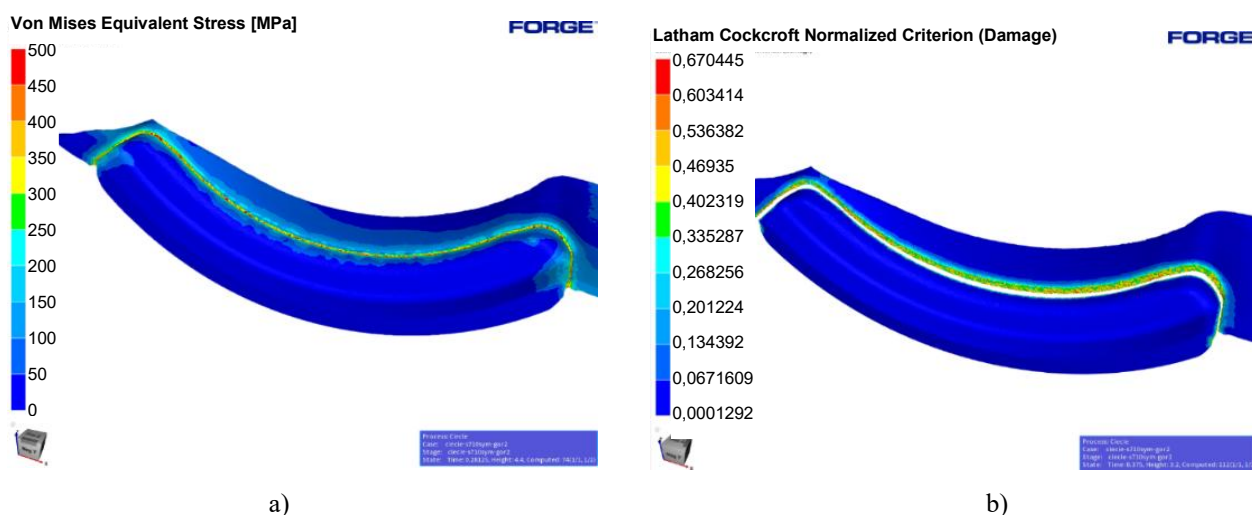


Fig. 18. Numerical simulation results with distributions: a) equivalent stresses at the final stage of cutting, b) temperature field: a) before trimming, b) after flash trimming

The analysis of the obtained results showed that the highest values of equivalent stresses during the hot trimming process, similar to those observed in the cold cutting process, are located along the cutting line. However, in this case, they reach maximum values of around 400 MPa. The distribution of the CL coefficient is similar, with the highest values located along the cutting line. Fig. 19 presents the cutting force courses for the hot trimming process.

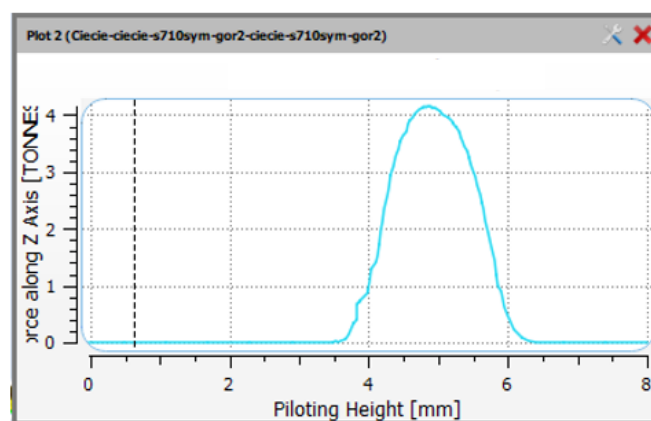


Fig. 19. Cutting force course for the part, hot trimming variant

The force diagrams show a significant difference in the maximum force values. The cutting force shown in Fig. 19 for the cold simulation is around 13 tons, while for the hot simulation, it is 4.2 tons. The cutting force in the hot simulation is three times lower than in the cold simulation for the adopted material models and fracture criterion. When comparing the maximum pressure values observed during hot and cold trimming, where the pressures for the cold process exceed 1000 MPa, it can be assumed that the 2.5 times lower pressure values and the 3 times lower cutting force should lead to a reduction in both energy consumption and tool wear. This will also positively affect the durability of the forging tools.

The conducted numerical simulations confirm the positive effect of using the hot trimming operation in terms of lower forces during the hot trimming process compared to the cold trimming process. This makes the process suitable for

verification under industrial conditions for the single-stage setup, and even for the four-stage hot trimming setup after forging, which will be the subject of further studies.

### 3.3. Verification of the hot trimming process in a single-stage setup under industrial conditions

The tools for the hot trimming process in a single-stage setup were then manufactured based on the previously developed CAD models. These tools were made from hot work tool steel, specifically 1.2344. The forgings were produced through the four-stage forging process followed by the hot trimming process in a single-stage setup. From the process, 28 forgings were collected, with 4 pieces (from one leaf) sampled every 100 units, and their measurements were taken. Fig. 20 shows the 3D scanning results from the bottom view for 4 representative forgings after trimming.

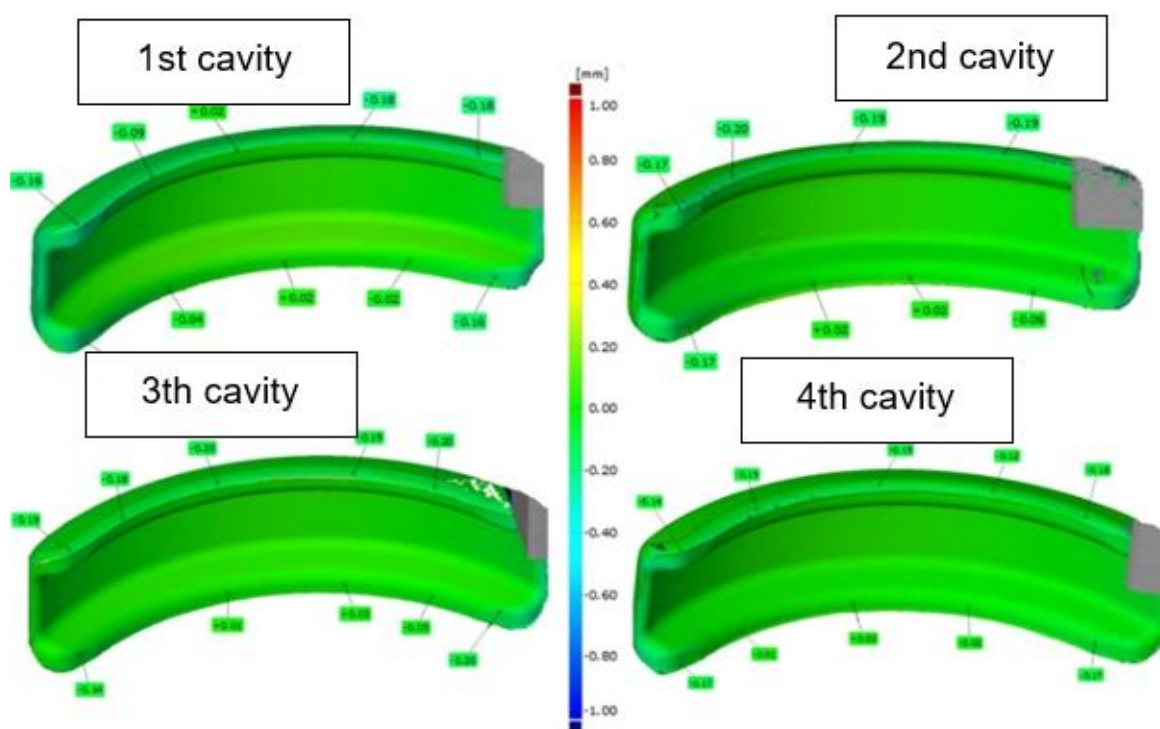


Fig. 20. 3D scanning result of forgings from individual seats – bottom view.

Based on Fig. 20, it can be observed that the largest shape errors occur for the forging from seat no. 3, reaching up to 0.2 mm. For seats 1, 2, and 3, the deviation does not exceed 0.18 mm for seat 1, 0.19 mm for seat 2, and 0.19 mm for seat 4, respectively. During the analysis of the deformations of the forgings after trimming from the top, no deviations greater than 0.05 mm were observed for all 4 seats.

In order to verify the developed heating system in terms of

quality, the adverse effect of scale and decarburization on the surface quality of forgings after hot trimming (directly after forging) at a temperature above 1100°C was examined and analyzed. Stainless steel is usually resistant to decarburization and scale formation under normal conditions. However, in certain extreme conditions, such as high temperature, it is possible to intensify these phenomena or other undesirable changes on the surface, which may be undesirable for elements



such as forgings intended for tank clamps. Therefore, in order to verify the dependencies in relation to the developed (new) solution, tests were carried out on the weight of scale on the

material surface, its type and the microstructure of the input material (Fig. 21) for 3 randomly selected forged elements (leaves).

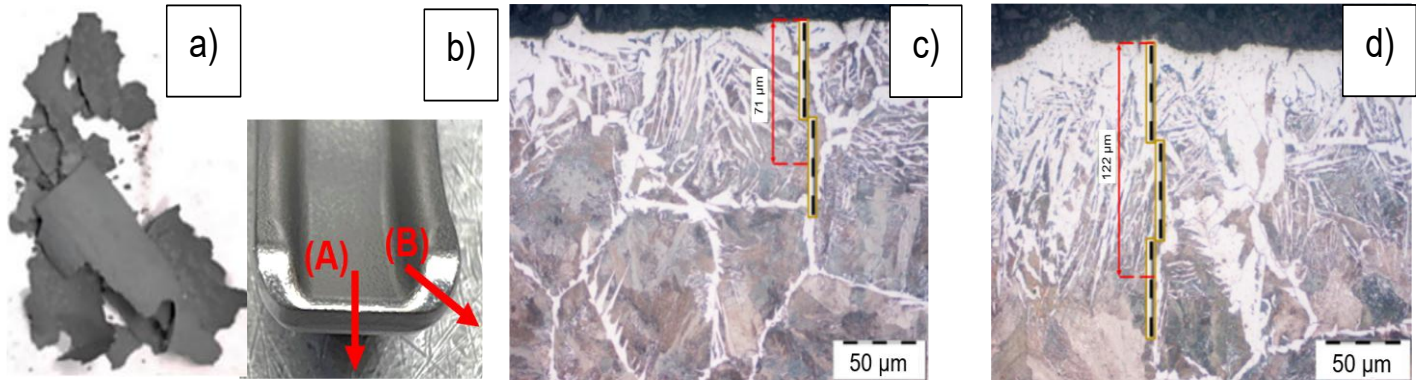


Fig. 21. Analysis of surface oxidation and decarburization of forged elements: a) the view of scale (oxide) from forged part (with for individual forgings), b) the view of sample with representative areas A and B, c) results of microstructural tests for A – area, d) for arm: B – area.

Then, the scale was removed from the entire forged element (containing 4 single forgings) before hot trimming in order to estimate the mass changes due to surface oxidation. The conducted test showed a surface-integrated scale with a thickness of 0.02–0.03 mm, where an average of 3–5 g of oxides was obtained, which was 0.3% of the total mass of the charge. The test was repeated twice, and the mass and thickness differences did not exceed 0.5% discrepancy. Microstructural tests of the surface were also carried out in two areas: (A) – in the longitudinal symmetry axis of the forging (Fig. 21c) and (B) – in the thickest part of the forging (from the inner radius in the transverse direction to the side surface – trimming line). The obtained results showed that the decarburization in the area (B) in the extreme case amounted to 120 µm (Figure 21d), while in the longitudinal axis in the area (A) the decarburization at the maximum point amounted to 70 µm. This phenomenon is extensively described and well-documented in the literature concerning high-temperature processing of stainless steels [46,47]. The values of the obtained decarburization are relatively small and within the permissible tolerance, so they do not pose a threat to the introduction of the hot trimming technology. As can be observed, the results of the hot trimming process in a single-stage setup achieved the intended effects, with products meeting the technical specifications and falling within the established dimensional and shape tolerances.

The needle-like microstructure observed on the surface of the tested samples (Fig. 21c,d) most likely resulted from local transformations occurring during the hot forging process and immediate hot trimming. Microhardness studies have shown that the hardness of this needle-like layer is close to or slightly lower than the core hardness, indicating that phase transformations do not lead to significant surface hardening. The hardness of all analyzed samples (15 pieces) was in the range of 171–188 HV. The condition of the analyzed forgings confirms the stability of the production process.

The following Table 3 presents the results obtained in terms of operational durability using hot trimming tools. The average durability is approximately 31 000 pieces, which is twice as long as for cold trimming tools. This further confirms the validity of implementing this solution under production conditions.

Table 3. Durability of hot flash trimming tools

No. of tool set	Operational durability (pcs)
1 <sup>st</sup> set	31 120
2 <sup>nd</sup> set	30 950
Average	31 035

In the case of starting the production process with new tools for cold forging and cold trimming as well as hot trimming, the process is as shown in Fig. 22.

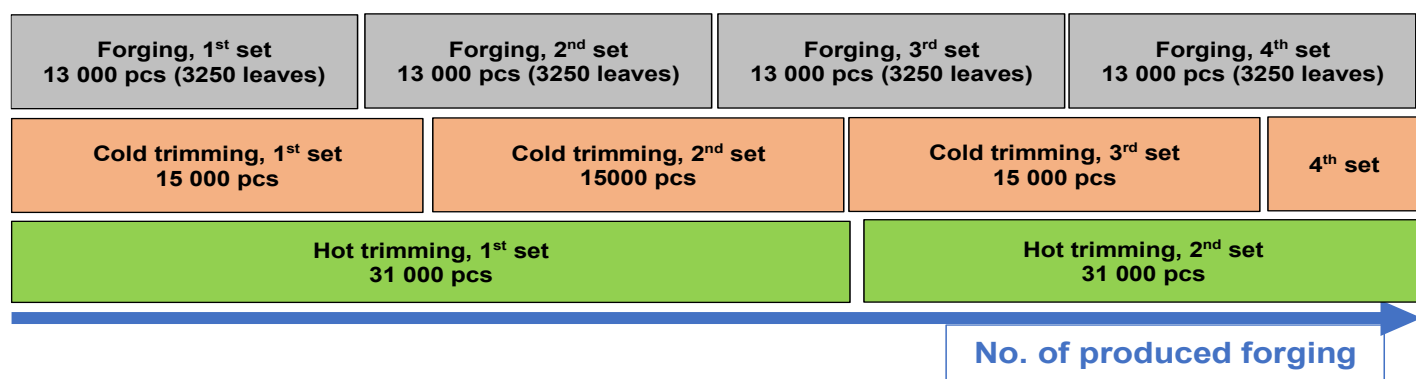


Fig. 22. Comparison of the operational durability for new forging, cold trimming, and hot trimming tools.

As shown in Fig. 22, it can be observed that the use of hot trimming tools, compared to cold trimming, not only offers significantly greater operational durability (i.e., 2 times higher) but also reduces preparation and finishing times. In the case of hot trimming tools, it is necessary to overhaul the flash trimming equipment half as often as for cold trimming, as illustrated in Fig. 22. This, in turn, leads to a reduction in both time and costs associated with implementing this solution.

In Table 4 below, both technologies analyzed in the study are compared, with particular emphasis and focus on cold trimming (current process) and hot trimming.

Table 4. Comparison of cold trimming and hot trimming.

Analyzed parameter	Cold trimming (current technology)	Hot trimming (new technology)
Tool material	K110	1.2344
Cutting forces	13 t	4,2 t
Dimension and shape accuracy	Max. 0.14 mm	Max. 0.2 mm
Average operational durability of the tool	15 587 pcs	31 035 pcs

As can be seen from the above Table 4, the new technology of hot trimming has two main advantages: lower cutting forces required during the process and significantly higher operational durability, approximately 2 times longer. In the case of hot trimming, we observe slightly wider dimensional deviations compared to cold trimming. However, these still fall within the established dimensional tolerances.

#### 4. Summary and conclusions

The paper presents the research results regarding the possibility of modifying the hot die forging technology with cold trimming to a process of forging followed directly by hot trimming for a

clamp-type component. The research was mainly conducted to analyze the effect of the technological change on the dimensional and shape accuracy of the forgings, as well as to increase process efficiency and enhance the operational durability of the trimming tools. The starting point was the forging process carried out in a four-stage setup and cold trimming in a single-stage setup. Both processes were performed manually. Therefore, numerical simulations were conducted for these processes, which allowed for a more comprehensive analysis of the forging and trimming technologies. These simulations confirmed that the existing technology (hot forging and cold trimming) was correctly planned. Furthermore, the numerical simulation results for direct hot trimming showed that the forces during trimming were 4.2 tons, while for cold trimming, they were approximately 13 tons. Von Mises stresses also indicated that the maximum cutting force in the hot trimming process was 400 MPa, which is 2.5 times lower compared to the cold trimming process. Additionally, it was determined that both the forging unit and the cold trimming press had sufficient power reserves, which were also confirmed under real conditions. Based on this, tools for hot trimming in a single-stage setup were developed, and technological trials were conducted. As a result of the industrial tests, forgings were produced, which were subsequently subjected to quality tests in the form of measurements of their dimensional characteristics. The measurement and analysis results showed that all the parameters for the forgings trimmed hot directly after the forging process were in compliance with the product's technical specifications. The accuracy slightly worsened by about 0.05 mm compared to cold trimming, but still remained within the tolerance field. At the same time, operational tests showed that the change in



technology allowed for an increase in the tool life from 15 000 to over 31 000 forgings. The key aspects of the technological modification have been presented in Table 4. The presented research results confirm that the hot trimming technology was correctly developed.

The conducted research and obtained results allowed for the formulation of the following conclusions:

- The study confirmed that alternative hot trimming, replacing cold trimming, does not negatively affect the dimensional and shape accuracy of the forgings.

- The operational durability of hot flash trimming tools is significantly greater than that of cold forging tools, as it increased more than twofold (compare Figures 7 and 22).

- It should also be noted that there are tangible aspects of production efficiency, as conducting the hot trimming process directly after forging increases productivity and shortens the overall manufacturing time. The increased durability of trimming tools reduces unit production costs and the need for more frequent tool changeovers.

- In the long term of operation, it is necessary to take into account the control of the extent of possible decarburization of

the forging surface and the influence of scale on the forged element during trimming, as this may result in increased wear of the trimming tools.

The conducted investigations also allows for the identification of further research directions:

- The studies have shown that it is possible to increase the number of forgings produced while meeting certain conditions for both cold and hot trimming processes. Therefore, further research should focus on increasing the number of forgings trimmed in a single stroke during the cold and/or hot trimming processes.

- It is also worth considering the use of the satisfactory results obtained in the context of potential changes in individual stages of the technological sequence in other processes. In some cases, the analysis of changes in the microstructure and operational properties of forgings after hot trimming, as opposed to cold trimming, may eliminate the need for an additional heat treatment stage, for example, by directly hardening the hot-trimmed forgings in water to achieve the required structure and/or hardness.

## References

1. Taylan A, Gracious N, Gangshu S. Cold and hot forging fundamentals and application, ASM International, Asm Metals Handbook 2005, 14: 337-338
2. ASM Metals Handbook, Vol. 14: Forming and Forging, Asm Intl, 1989
3. ISO GPS 10360-4:2000 Geometrical Product Specifications (GPS) – Acceptance and Reverification Tests for Coordinate Measuring Machines (CMM) – Part 4: CMMs used in Scanning Measuring Mode.
4. Ling-min LIAO, Chun-xu PAN, Yu MA. Manufacturing techniques of armor strips excavated from Emperor Qin Shi Huang's mausoleum, China. Transactions of Nonferrous Metals Society of China, 2010, 20(3): 395-399. [https://doi.org/10.1016/S1003-6326\(09\)60152-7](https://doi.org/10.1016/S1003-6326(09)60152-7)
5. Douglas R, Kuhlman D. Guidelines for precision hot forging with applications, Journal of Materials Processing Technology, 2000, 98(2): 182-188. [https://doi.org/10.1016/S0924-0136\(99\)00197-1](https://doi.org/10.1016/S0924-0136(99)00197-1)
6. Milutinović M, Vilotić D, Movrin D. Precision forging—tool concepts and process design. J Technol Plasticity 2008, 33:73–89
7. Steffens K, Wilhelm H. Next engine generation: materials, surface technology, manufacturing process. MTU Aero Engines Report 2003:1–17
8. Bendjoudi Y, Becker E, Bigot R, Amirat A. Contribution in the evaluation of a performance index of hot forging dies. International Journal of Advanced Manufacturing Technology 2017, 5-8: 1187-1201. <https://doi.org/10.1007/s00170-016-8829-4>
9. Kumar D, Mondal S. A Review on Modelling, Design and Optimization of Forging Process, 2020, IOP Conf. Ser.: Mater. Sci. Eng. 1126, 012001. <https://doi.org/10.1088/1757-899X/1126/1/012001>
10. Avetisyan M, Meinders T, Huetink J. Improvement of springback predictability after forming and trimming operations. In: Proceedings of the seventh Esaform conference on material forming, Trondheim, Norway 2004.
11. Chen Z.H, Tang C.Y, Lee T.C. An investigation of tearing failure in fine-blanking process using coupled thermo-mechanical method. International Journal of Machine Tools and Manufacture 2004, 44: 155–65. <https://doi.org/10.1016/j.jmachtools.2003.10.010>
12. Bouissa Y, Bohlooli N, Shahriari D, Champliand H, Morin J.B, Jahazi M. FEM modeling and experimental validation of quench-induced

- distortions of large size steel forgings. *J. Manuf. Process.* 2020, 58: 592–605. <https://doi.org/10.1016/j.jmapro.2020.08.042>
13. Lee S, Kim K, Kim N. A Preform Design Approach for Uniform Strain Distribution in Forging Processes Based on Convolutional Neural Network. *Journal of Manufacturing Science and Engineering-Transactions of The ASME.* 2022, 144(12): 121004. <https://doi.org/10.1115/1.4054904>
  14. Lisiecka-Graca P, et al. Evaluation of cracking risk of 80MnSi8-6 nanobainitic steel during hot forging in the range of lower temperature limits. *Materials Science-Poland* 2024, (42)1, pp. 171-185. <https://doi.org/10.2478/msp-2024-0011>
  15. Favi C, et. al. Key features and novel trends for developing cost engineering methods for forged components: a systematic literature review. *The International Journal of Advanced Manufacturing Technology* 2021, 117:2601–2625. <https://doi.org/10.1007/s00170-021-07611-4>
  16. Musel T, Young W.A, Judd R, A rule-based approach to predict forging volume for cost estimation during product design. *The International Journal of Advanced Manufacturing Technology* 2010, 46(1): 31-41. <https://doi.org/10.1007/s00170-009-2108-6>
  17. Dieter G.E, Kuhn H.A, Semiatin S.L, Eds.; *Handbook of Workability and Process Design*, ASM International: Materials Park, OH, 2003, ISBN 978-0-87170-778-9
  18. Kitayama S, et. al. Numerical and experimental investigation of process parameters optimization in hammer forging for minimizing risk of crack, *Journal of Advanced Mechanical Design Systems and Manufacturing*, 2024, AN: 2400059. <https://doi.org/10.1299/jamdsm.2024jamdsm0087>
  19. Park J, Lee J, Shin H. Integrated reliability assessment method for forging systems based on process variability. *International Journal of Advanced Manufacturing Technology*, 2020, 109(9–12), 2641–2653. <https://doi.org/10.1007/s00170-020-05825-y>
  20. Morinaga Y, Hirota K. Reliability assessment of high-temperature forming equipment using data-driven degradation models. *Mechanical Systems and Signal Processing* 2021, 154, 107546. <https://doi.org/10.1016/j.ymssp.2020.107546>
  21. Behrens BA, Doege E, Reinsch S, Telkamp K, Daehndel H, Specker A. Precision forging processes for high-duty automotive components. *J Mater Process Technol* 2007, 185:139–146. <https://doi.org/10.1016/j.jmatprotec.2006.03.132>
  22. Gao Z, Wanyama T, Singh I, Gadhri A, Schmidt R. From industry 4.0 to robotics 4.0—a conceptual framework for collaborative and intelligent robotic systems. *Proced Manuf.* 2020, 46:591–9. <https://doi.org/10.1016/j.promfg.2020.03.085>
  23. Hawryluk M, et. Al. Analysis of the impact of forging and trimming tools wear on the dimension-shape precision of forgings obtained in the process of manufacturing components for the automotive industry. *Eksplotacja i Niezawodność – Maintenance and Reliability* 2019, 21 (3): 476–484, <http://dx.doi.org/10.17531/ein.2019.3.14>
  24. Hilditch TB, Hodgson PD. Development of the sheared edge in the trimming of steel and light metal sheet, Part 1—experimental observations. *J MaterProces Technol* 2005, 169:184–91. <https://doi.org/10.1016/j.jmatprotec.2005.02.266>
  25. Hilditch TB, Hodgson PD. Development of the sheared edge in the trimming of steel and light metal sheet, part 2—Mechanisms and modelling. *J MaterProces Technol* 2005, 169:192–998. <https://doi.org/10.1016/j.jmatprotec.2005.02.267>
  26. Lu B, Ou H, Armstrong CG. A simple method to evaluate trimming operation on hot forged blade components. In: *Proceedings of the 15th UK conference of the ACME*, Glasgow, UK, 2006.
  27. Li M. An experimental investigation on cut surface and burr in trimming aluminium autobody sheet. *International Journal of Mechanical Sciences* 2000, 42: 889–906. [https://doi.org/10.1016/S0020-7403\(99\)00033-8](https://doi.org/10.1016/S0020-7403(99)00033-8)
  28. Kim T, et. al. A New Mechanical Cold Trimming Process Assisted by Dashed Lined Infrared Heat Treatment of Martensitic Steel Considering Energy Efficiency, *International Journal of Precision Engineering and Manufacturing-Green Technology* 2023, 10: 1447–1468. <https://doi.org/10.1007/s40684-022-00427-x>
  29. Bulzak T, Tomczak J, Pater Z. A comparative analysis of hot and cold flashless forging of a stepped shaft using vertically-parted dies, 2021, 116: 2521–2530. <https://doi.org/10.1007/s00170-021-07542-0>
  30. Kacaturk F, et. al. Optimization of trimming process in cold forging of steel bolts by Taguchi method. *International Journal of Pressure Vessels and Piping*, 2021, 194 (A), AN: 104503. <https://doi.org/10.1016/j.iipvp.2021.104503>
  31. Choi W-Y, Kwak D-Y, Son I-H, Im Y-T. Tetrahedral mesh generation based on advancing front technique and optimization scheme. *International Journal for Numerical Methods in Engineering*, 2003, 58: 1857–72. <https://doi.org/10.1002/nme.840>
  32. Dhondt G. A new automatic hexahedral mesher based on cutting. *International Journal for Numerical Methods in Engineering* 2001, 50: 2109–26. <https://doi.org/10.1002/nme.114>

33. Lu B, Ou H. An efficient approach for trimming simulation of 3D forged components. *International Journal of Mechanical Sciences* 2012, 55(1): 30–41. <https://doi.org/10.1016/j.ijmecsci.2011.11.013>
34. Guoqun Zhao, Xinwu Ma, Xinhai Zhao, Ramana V. Grandhi, Studies on optimization of metal forming processes using sensitivity analysis methods, *Journal of Materials Processing Technology*, Volume 147, Issue 2, 2004, Pages 217–228, ISSN 0924-0136, <https://doi.org/10.1016/j.jmatprotec.2003.12.018>
35. Zhang W, Peng Y. Probabilistic failure analysis in hot forming simulations: an integrated FEA and machine learning approach. *Journal of Manufacturing Processes*, 2023, 86, 245–253. <https://doi.org/10.1016/j.jmapro.2023.02.014>
36. Cockcroft M.G, Latham D.J. Ductility and the workability of metals. *Journal of the Institute of Metals* 1968, 96: 33–9
37. Goijaerts A.M, Givaert L.E, Baaijens F.P.T. Evaluation of ductile fracture models for different metals in blanking. *Materials Processing Technology* 2001, 110: 312–23. [https://doi.org/10.1016/S0924-0136\(00\)00892-X](https://doi.org/10.1016/S0924-0136(00)00892-X)
38. Kiener C, Neher R, Merklein M. Influence of tribological conditions on cold forging of gears. *Production Engineering* 2018,12-3: 367–375. <https://doi.org/10.1007/s11740-017-0785-9>
39. Lin Y.C, Chen D.D, Chen M.S, Chen X.M, Li J. A precise BP neural network-based online model predictive control strategy for die forging hydraulic press machine. *Neural Computing and Application* 2018, 29: 585. <https://doi.org/10.1007/s00521-016-2556-5>
40. Lu B, Ou H. An efficient approach for trimming simulation of 3D forged components. *International Journal of Mechanical Sciences* 2012. <https://doi.org/10.1016/j.ijmecsci.2011.11.013>
41. Hawryluk M., et. al. Influence of the nitriding process on the durability of tools used in the production of automotive forgings in industrial hot die forging processes on hammers. *Materials Science-Poland*, 2024, 42(4): 1–18. <https://doi.org/10.2478/msp-2024-0047>.
42. Kozłowski E, Borucka A, Oleszczuk P, Leszczyński N. Evaluation of readiness of the technical system using the semi-Markov model with selected sojourn time distributions. *Eksploracja i Niezawodność – Maintenance and Reliability*, 2024, 26(4):191545. <https://doi.org/10.17531/ein/191545>
43. Zhou S, Ma X, Wang J, Chen Y, Yang L. Global-dynamic maintenance management of multi-component degrading plants with non-immediate replacement: a self-adaptive grouping approach. *Eksploracja i Niezawodność – Maintenance and Reliability*, 2025, 27(1):193132. <https://doi.org/10.17531/ein/193132>
44. Ighravwe DE, Oke SA, Adebisi KA. Reliability-based maintenance technicians' workloads optimisation model with stochastic consideration. *Journal of Industrial Engineering International*, 2015. <https://doi.org/10.1007/s40092-015-0134-6>
45. Lachowicz M. Insight into the microstructural stability and thermal fatigue behavior of nitrided layers on martensitic hot forging tools. *Materials Science-Poland*, 2025, 43(1): 1-17. <https://doi.org/10.2478/msp-2025-0005>
46. Zurek, J., Cosler, H., Quadackers, W.J. et al. Effect of Surface Oxide on Decarburization Reaction in the Austenitic Steel S304H. *High Temperature Corrosion of mater.* 100, 491–523 (2023) <https://doi.org/10.1007/s11085-023-10196-w>
47. Sabioni, A.C.S., Ramos, R.P.B., Ji, V., Jomard, F., 2012. Oxygen Diffusion Study in Oxidation Films of the AISI 304 Austenitic Stainless Steel. *DDF*. <https://doi.org/10.4028/www.scientific.net/ddf.323-325.345>